

A Modeling Study of Atmospheric Transport and Photochemistry in the Mixed Layer during Anticyclonic Episodes in Europe. Part I: Meteorology and Air Trajectories

H. VAN DOP AND J. F. DEN TONKELAAR

Royal Netherlands Meteorological Institute, 3730 AE De Bilt, The Netherlands

F. E. J. BRIFFA

Shell International Petroleum Company, London SE1 7NA, England

(Manuscript received 18 October 1986, in final form 23 March 1987)

ABSTRACT

A climatological study has been carried out of the occurrence and properties of a large number of dry and sunny spells in recent summers (1976–83). The frequency of the spells, which are very favorable for atmospheric photochemical activity, were found to be significantly higher in the investigated period than in previous years. A detailed examination of 25 episodes has been carried out. During the episodes, 72 h back trajectories have been computed, and information provided on temperature, humidity, cloud cover and inversion height. The trajectories, determined at different altitudes for five receptor locations [Soltau, Freiburg (FRG), De Bilt (Netherlands), Soissons, Nancy (France)] in Europe, show a predominance for advection from eastern to western Europe. For the two more northerly European locations [Soltau (FRG) and de Bilt (the NL)], the air trajectories also pass over less densely populated or maritime regions. Ozone concentrations, recorded at a station in the Netherlands, are examined in relation to the direction of the arriving air mass.

1. Introduction

Some 10 years have passed since the observation of unusual damage to firs in West Germany. The forest decline reported has been ascribed to a variety of factors including climatological influences (drought, frost, etc.) and air pollution. The atmospheric pollutants suspected of playing a role are sulphur dioxide, nitrogen oxides and photo-oxidants. The extent to which these atmospheric pollutants contribute to the damage is still uncertain and a matter of continuing research in many countries (Miller and McBride, 1975; Smith, 1981; Ulrich et al., 1980; Johnson and Siccama, 1983). Emission reductions are costly; moreover, the reduction of sulphur dioxide emissions requires a different abatement strategy from that for the reduction of nitrogen oxides or the precursors (hydrocarbons and nitrogen oxides) of photo-oxidants. Photo-oxidants are formed in the atmosphere and since the occurrence of high photo-oxidant concentrations is strongly related to fair weather periods, the pattern of western European climate, over the last decade, also needs to be examined. The meteorological aspects are presented and discussed herein (Part I), while in the Part II study (Selby, 1987; hereafter referred to as Part II) a photochemical model is described which estimates ozone levels in Western Europe.

High photo-oxidant levels are most likely during dry, warm and sunny weather periods in the summer season (Cox et al., 1976; Guicherit and Van Dop, 1977;

Guicherit, 1978). Such periods are characterized by persistent anticyclonic circulation over Europe. The photochemical model computations were directed at estimating the ozone levels reached at selected receptor locations. Two of the locations chosen are in forested regions, Freiburg, near the Black Forest in southwest Germany, and Nancy (northeast France). Two other locations are situated in agricultural regions, Soltau (north Germany) and Soissons (northwest France). The fifth location, (Cabauw) near De Bilt in the Netherlands, serves a reference function, since locally recorded ozone (O_3) concentrations are available. To investigate the presence of high O_3 levels, we have examined the appropriate meteorological parameters such as air mass advection, the weather at the receptor locations, temperature, and the diurnal variability of the mixing height along the air trajectories.

A trajectory is defined as the path of an air parcel or particle in an airstream when it assumes the velocity of the surrounding fluid. In the atmosphere, this concept is often used when only the horizontal motions of a particle are considered.

First a selection was made of fair weather episodes (section 2). Trajectories along which air was transported towards the chosen receptor sites (section 3) were then determined. Finally, the weather data associated with the trajectories, namely, cloud cover, maximum temperature, minimum temperature, dewpoint (humidity) and mixing height have been summarized in section 4.

Information on the causes of reported forest damage,

TABLE 1. Fair weather episodes of at least three consecutive days in Europe during the summers of 1976–83. The bottom row denotes the total number of such fair weather days in each summer.

1976	1978	1979	1980	1981	1982	1983	
5 May–9 May	26 May–5 June	13 May–16 May	30 Apr.–4 May	11 Aug.–15 Aug.	10 May–15 May	6 June–24 June	
6 June–15 June	23 July–31 July	1 June–5 June	9 May–19 May	2 Sept.–7 Sept.	29 May–10 June	8 July–18 July	
18 June–17 July	18 Aug.–27 Aug.	17 June–21 June	3 June–6 June		8 July–15 July	14 Aug.–31 Aug.	
7 Aug.–30 Aug.		26 Aug.–1 Sept.	22 July–3 Aug.		8 Sept.–20 Sept.		
69	30	19	33	11	40	48	= 250

albeit considerable, is still uncertain. Included along with the various causes mentioned is the long, dry, and hot summer of 1976.

The present study has been restricted to recent summer periods and, given the lifetime of circa 5 years for pine needles, covers the years 1978–83, as well as the summer of 1976.

2. Analysis of dry, sunny spells

The identification of periods with dry, warm and sunny weather over a large part of the European continent was obtained by carrying out a survey of the weather pattern. Since the model described in Part II involves the chemical reactions during at least three consecutive warm and sunny days, the following considerations were then used to select the episodes for the computed air trajectories:

- Episodes with a minimum length of three days;
- Similarity of weather conditions over the advection areas during the episodes;
- Maximum temperatures preferably $>20^{\circ}\text{C}$ on the three consecutive days;
- Maximum mixing height to be <2000 m, or preferably <1600 m, for both receptor locations and along the trajectories;

- The selection to be from the summer months of May to September inclusive.

A selection according to these considerations would include days on which photochemical air pollution is expected to occur over large parts of West and Central Europe (Guicherit and Van Dop, 1977). To minimize the influence of weather variables on the results from photochemical computations, similar weather conditions at the five receptor locations and along the trajectories were chosen. In this way, the results reflect to a large extent the relationship between the emissions picked up and the ozone levels along the trajectories.

An investigation of the 3 h surface weather maps for the total period of 1071 days yielded the results shown in Table 1. The total number of fair weather days on the West European continent—involved in episodes of at least 3 days—was 250. For each day, the type of large-scale weather circulation (“Groszwetterlage”) was determined (Hess and Brezowski, 1969) (Table 2, column C). About 90% of the days were characterized by anticyclonic weather.

In the first column (A) of Table 2, the climatologically normal (1949–80) distribution of large-scale weather circulations is presented, and in column B the distribution during the summers of 1976 and 1978–83. It is noteworthy that in the investigated period,

TABLE 2. Frequency of occurrence (in %) of large scale weather patterns (Hess and Brezowski, 1969).

		A	B	C	D
	A. According to the climatology of the period 1949–80				
	B. For the summers (May–September) of 1976, 1978–83.				
	C. For the selection of 250 warm dry and sunny days (cf. Table 1)				
	D. For the final selection of 25 episodes.				
HM	Anticyclone over Central Europe	6	7	18	25
BM	Ridge of high pressure over West and Central Europe	8	11	15	20
HNFa	Anticyclone over Scandinavia and the NE Atlantic with anticyclonic circulation over Central Europe	1	3	12	5
HFa	Anticyclone over Finland and Scandinavia with anticyclonic circulation over Central Europe	3	4	12	14
HNa	Anticyclone over the NE Atlantic with anticyclonic circulation over Central Europe	3	2	4	9
NEa	Anticyclonic NE circulation over Central Europe	3	4	9	8
HB	Anticyclone over the British Isles and the North Sea	3	3	5	4
Sa, SEa	Anticyclonic circulations from the S or SE	2	3	4	5
SWa, NWa, Wa, Na	Anticyclonic circulations from the SW, NW, W or N	13	13	10	7
	Various cyclonic circulations	58	50	11	3

TABLE 3. Duration of consecutive fair weather episodes longer than 3 days during the summers 1976, 1978, 1983. The number of selected episodes for the Part II study is indicated in parentheses. For example, the fourth spell in 1982, is denoted by 13(2), which means that the spell has a length of 13 days and that from this spell 2 episodes are selected.

Year	Spell length in days				Yearly total
1976	5(0)	10(1)	30(3)	24(2)	69(6)
1978	11(1)	9(1)	10(1)		30(3)
1979	4(0)	5(0)	5(0)	5(1)	19(1)
1980	5(0)	11(1)	4(0)	13(1)	33(2)
1981	5(1)	6(1)			11(2)
1982	6(0)	13(2)	8(1)	13(2)	40(5)
1983	19(2)	11(1)	18(3)		48(6)
Total					250(25)

anticyclonic circulations had a stronger than normal prevalence (50% vs 42%). It is not surprising that due to the selection made, anticyclonic circulation types start to prevail.

Table 3 shows the selection of 25 episodes suitable for the Part II study. Table 4 reviews these episodes together with a listing of the circulation types. Here only 30% of the circulation types had a cyclonic character (Table 3, column D).

The highest frequencies are for weather categories HM (25%), BM (20%), HF_a + HNF_a (19%), and HN_a (see Table 2). In a study of photochemical oxidants over northwestern Europe during 1976–79, Schjoldager et al. (1981) related high ozone concentrations to the type of weather circulation. One of the conclusions was that although high ozone levels are strongly associated with some weather categories (e.g., HM, BM, HN_a, HF_a and HNF_a) the majority of these weather types did not necessarily imply high ozone concentrations. It seems that the large-scale weather pattern alone does not determine sufficient conditions for ozone formation. The category HM was, however, associated with high ozone concentrations in Great Britain and the European continent during 16 days out of a total of 27 days.

Becker et al. (1979) reported on a series of studies in the Cologne/Bonn area in 1975–78. For the episode in June–July 1976, their conclusion was similar to that of Cox et al. (1976), namely, that local emissions, in addition to the large-scale weather pattern and transport, contributed significantly to the ozone levels.

3. Trajectory calculations

Trajectory analysis is a powerful tool for describing the long-range transport of pollutants and for determining ambient concentrations and deposition in complex source areas (Pack et al., 1978). Initially, the transport (linear), chemistry, and deposition of sulphur dioxide emissions were treated by trajectory or La-

grangian models (Eliassen and Saltbones, 1983), but more recently the transport of chemically reactive compounds has also been similarly described (Bottenheim et al., 1984; Schjoldager et al., 1985; Rodhe et al., 1982; Hov et al., 1983). A key assumption in all these models is that horizontal transport describes the motion of an air parcel whose dimensions extend upwards to 1000 m but with horizontal dimensions of 100–200 km. Although the air parcel is large enough not to be distorted by the (nonuniform) flow field, the horizontal exchange is neglected. The effects of cloud venting on the boundary layer or boundary layer entrainment of cleaner air from the troposphere may be important under certain conditions. However, since the study is related to cloudless or practically cloudless weather situations and as the top of the mixing layer in the anticyclonic circulation systems is characterized by a subsidence inversion, the vertical exchange may also be neglected. The assumptions made indicate the limitations of trajectory models, since the lack of spatial resolution hampers an accurate quantitative description of atmospheric chemical processes. In addition, as described later, the nonuniformity of the flow field, together with the actually variable height of the mixed layer, makes it difficult to determine the sources that contribute to a traveling air parcel. Nonetheless, trajectory models are as yet unique in obtaining a quick insight to atmospheric transport features. Complex, more realistic and detailed models are only operational

TABLE 4. Classification of the 25 selected episodes. Numbers in parentheses denote the days with a given circulation type, i.e., the Groszwetterlagen, over West and Central Europe.

Episode	Date	Circulation*
1	6–9 May 1976	(4 SE _a)
2	11–14 June 1976	(2 HNF _a , 2 HF _a)
3	25–28 June 1976	(3 BM, 1 BW ₂)
4	4–7 July 1976	(4 HN _a)
5	7–10 Aug. 1976	(4 NE _a)
6	23–26 Aug. 1976	(1 HF _a , 3 HM)
7	29 May–1 June 1978	(2 NE _a , 2 HM)
8	27–30 July 1978	(4 HF _a)
9	19–22 Aug. 1978	(4 BM)
10	29 Aug.–1 Sept. 1979	(4 HM)
11	11–14 May 1980	(4 HF _a)
12	22–25 July 1980	(4 HM)
13	12–15 Aug. 1981	(2 NE _a , 2 W _a)
14	3–6 Sept. 1981	(1 HN _a , 3 HM)
15	31 May–3 June 1982	(3 HM, 1 SE _a)
16	7–10 June 1982	(4 HN _a)
17	10–13 July 1982	(1 HM, 3 HF ₂)
18	9–12 Sept. 1982	(4 BM)
19	14–17 Sept. 1982	(1 BM, 3 HM)
20	17–20 June 1983	(4 HB)
21	9–12 July 1983	(1 HF ₂ , 3 HNF _a)
22	13–16 July 1983	(3 NW _a , 1 T _r W)
23	16–19 Aug. 1983	(2 SW _a Y, 2 HM)
24	24–27 Aug. 1983	(4 BM)
25	28–31 Aug. 1983	(4 BM)

* Number of days with given circulation type.

on a modest scale and more expensive with regard to computer time.

The present study has been directed at an analysis of a number of trajectories at various altitudes. For each of the 25 episodes, the computed trajectories reach the receptor locations at the end of the episode. The selected time of arrival is 1500 or 1600 UTC. At this time of day, the mixing layer will have reached its maximum height during warm and sunny days. Moreover, diurnal O_3 concentrations reach their peak values at about the same time.

The air trajectories, tracked back over 3 days (72 hours), also start at 1500 or 1600 UTC. During the time that the air is well mixed (up to a height 1600–2000 m), air transport for the whole of the mixed layer occurs, but during the evening and night, when vertical exchange is often restricted to an altitude of 200 m, the air which is transported at higher levels becomes “decoupled” from the shallow layer. The air mass associated with each layer will generally follow different

trajectories, since the variation of wind speed and direction between the two layers is large during the nighttime.

As a result of the diurnal variation in the stability and the depth of the mixing layer, difficulties can arise with determining the source areas that contribute to the air mass arriving at the receptor locations (Fig. 1). Clearly it is only when the transport velocities at different altitudes up to 1500 m do not vary significantly (i.e., when trajectories, determined at different heights approximately coincide) that the relevant sources of emission are those positioned along the same trajectory. When the surface trajectory does not coincide with that at a higher altitude, it is reasonable to assume that other sources, situated in the region enclosed by both trajectories, will make a contribution. It is, however, difficult to determine the exact emissions contribution from all the other sources (see Fig. 1). These influences are further addressed in subsection 3b on coherence.

To examine the “coherence” of the 25 selected ep-

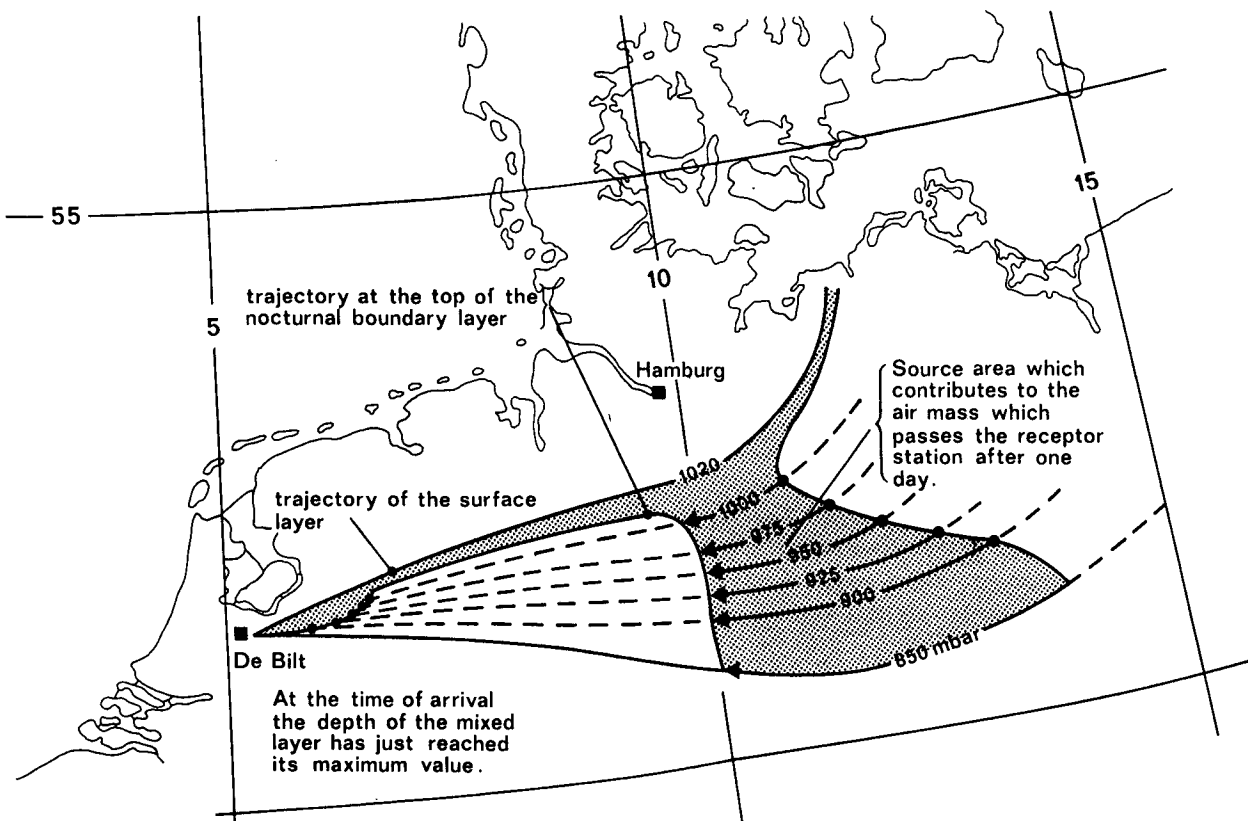


FIG. 1. Illustration of the contribution made by different trajectories passing over a source area to the air mass reaching a receptor location after 1 day. In general, the trajectories for different pressure levels will follow different pathways. The emissions picked up are from different regions of the source area. The dashes show the start of the trajectories which during daytime are contained in the mixing layer. The arrows indicate the end of the trajectories. Due to the gradual evolution in time of the mixing layer, the starting time of the 1000 mb trajectory is earlier than that for the 975 mb trajectory, etc. The arrows end, however, at practically the same time since the mixed layer breaks down within approximately 1 h of sunset. Due to the greater windspeed at higher altitudes, the enclosed part of the 850 mb trajectory will be larger than that for the lower pressure levels, in spite of the somewhat smaller time period during which it is included in the mixing layer. The receptor location is reached when the boundary layer has again reached its maximum height on the following day. As the boundary layer increases in height, it is the lower-level trajectories that first begin to mix.

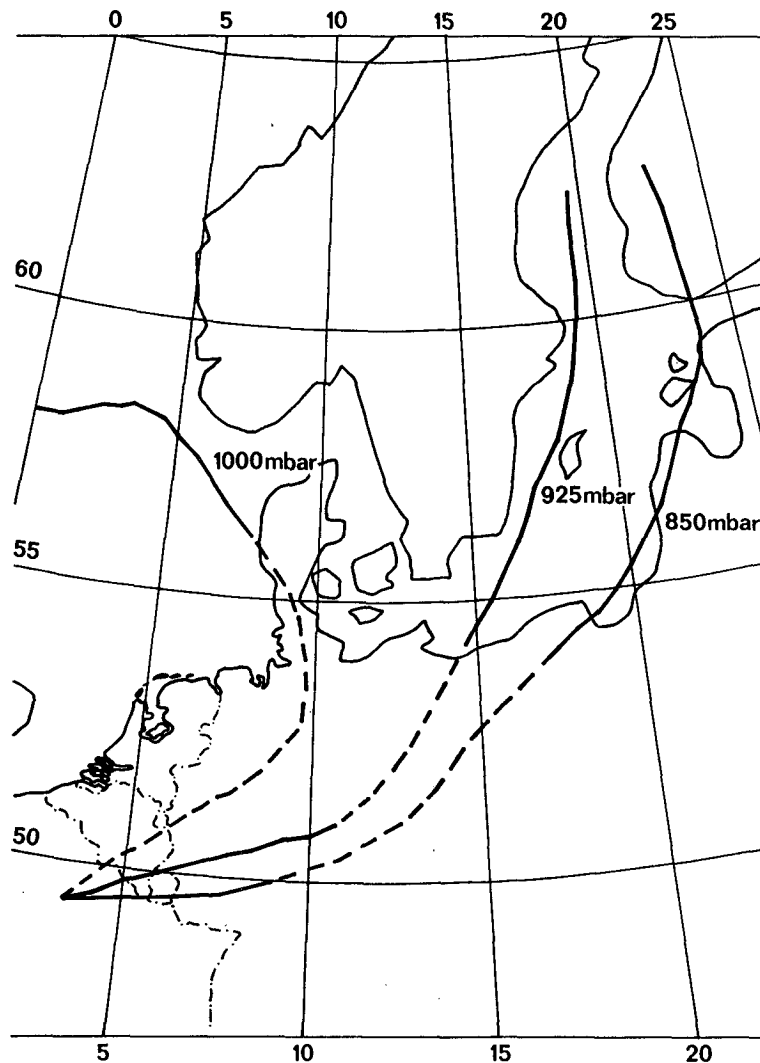
isodes, trajectories were computed at three levels within the mixed layer. The 850 mb level, which corresponds to an altitude of about 1500 m, and is one of the standard atmospheric levels in meteorology, was chosen for the highest level of trajectory calculation.

Generally speaking, the air arriving at a receptor location will have picked up atmospheric emissions from anywhere within the area enclosed between the 850 and 1000 mb trajectories (near ground surface) associated with the same starting and receptor sites. The matter of choosing the most representative trajectory for each episode depends mainly on the diurnal variation of the mixing height, and the divergence between surface and upper air trajectories. During the period

between ca. 1700 to 0600 UTC, the surface trajectory is the most representative but during the daytime, air along the surface trajectory mixes and merges with the air layers between 200 and 2000 m (cf., Fig. 1b).

The 925 mb trajectory may be taken as representing an average trajectory with respect to the source locations. The latter intermediate level trajectory is usually situated in the sector between the 850 and 1000 mb trajectories and corresponds to a height of about 600 m.

For episodes during 1980, 1981, 1982 and 1983 (15 cases), trajectories were computed with the Royal Netherlands Meteorologisch Instituut (KNMI) trajectory model (Reiff et al., 1984), which uses the meteo-



Soissons
 Time of departure 17 - 06 - 83 1600 GMT
 Time of arrival 20 - 06 - 83 1600 GMT

FIG. 2. Air trajectories ending at Soisson (France). Numbers along the trajectory denote barometric pressure. Ascending trajectories are represented with dashes.

rological data collected at the European Centre for Medium Range Weather Forecasting (ECMWF) in Reading. The KNMI model computes the 1000, 925, and 850 mb trajectories arriving at a receptor location. Since the model allows for vertical motions, pressure values along the trajectories may vary, and in effect the trajectories are not constant pressure level trajectories. An example of a trajectory calculation is shown in Fig. 2. Since the ECMWF data could only be used for trajectories from 1980 onwards, the trajectories for the remaining 10 episodes were obtained from weather chart analysis. Often a trajectory will cover a considerable distance but during stable weather situations with little advection, the trajectory length can be much shorter.

a. Origin of air masses

It is useful to examine the directional origin of air trajectories and note whether "sectors of preference" are associated with given receptor locations. The procedure adopted required all surface (1000 mb) and 850 mb trajectories, associated with a given receptor point, to be plotted on separate charts. By placing an overlay with eight wind direction sectors on each of the charts, the predominant direction associated with the arriving trajectories was then determined. The results for the different locations are summarized in Figs. 3 and 4. Figure 3 shows that the surface trajectories of Soissons, Nancy and Freiburg (52%) have a strong preference for the NE-E sector. The preference is less pronounced for the 850 mb trajectories, although the fraction of the higher trajectories situated in the sector between north and east is also about 70%.

The surface trajectories for Soltau and de Bilt do not show any directional preference. The sector between NE and E contains only 16–24% of the trajectories.

Unlike Soltau and de Bilt, Soissons, Nancy and Freiburg show a preference for northeasterly advection. Another striking feature is the absence of trajectories in the sectors SE-SW for all locations (cf., Fig. 4). On a more general level, it is noted that these preferences are not only a feature of the particular episodes selected but also have a general validity for the weather patterns identified.

b. Coherence and stagnancy of surface and upper-air trajectories

The coherence between the advection directions of air at different heights in the boundary layer, especially during the daytime period, is discussed in this subsection. In the context of this study, only a very general definition of "coherence" is used. The qualifications developed are only descriptive in nature. When the area between the 1000 and 850 mb trajectory is within a sector of less than about 20°, the term "good coherence" is used. A similar approach is taken for qualifications like "moderate" and "poor" coherence. When

the sector for the enclosed area is judged to be large, the coherence is described as "poor".

Similar considerations are used for describing the stagnancy of the weather type. When the trajectories are "short," the weather is stagnant and when they are "long," there is no stagnancy. Intermediate cases are classified as "moderate". An overview is given in Table 5. The following conclusions may be drawn:

- The number of conditions with "good", "moderate", and "poor" coherency is roughly similar for the various locations.
- The stagnancy is low for Soltau and de Bilt when compared with Freiburg.
- The total number of stagnant weather conditions is small: 3–9 episodes.

When both the coherency and stagnancy of the 25 episodes are examined, the conclusion is that good coherency occurs when there is moderate or no stagnancy. Also, during stagnant weather conditions, the trajectories have no clear preference for any of the three coherence classes.

4. Weather elements along the trajectories

The variability of the relevant meteorological parameters of the 25 selected episodes are further examined. To model the atmospheric chemistry along an air trajectory, it is necessary to specify a number of relevant meteorological parameters associated with a chosen trajectory. The meteorological parameters required (for Part II) are the diurnal variation along the surface trajectory of

- mixing height,
- air temperature near the earth surface (observation height),
- humidity,
- cloudiness.

a. The mixing height

The maximum mixing height is usually determined from the vertical temperature and humidity profile of the 1200 UTC radiosonde ascent, and the afternoon maximum temperature at the sites over which the trajectory passes at about 1300–1400 UTC (Holzworth, 1967). Additional useful information is the type, the height of the base, and the amount of the convective cloud over the trajectory path. For the present study, radiosonde ascents along and close to the trajectories were used, in combination with data on cloud cover provided on surface weather maps. Since 25 rather similar weather conditions were selected, the diurnal variations of mixing height presented similar results.

The mixing heights for the first ten episodes were determined at 6 h intervals, i.e., at 0300, 0900, 1500 and 2100 UTC, and, in some cases, also at 0000, 0600, 1200 and 1800 UTC. An average curve of the diurnal

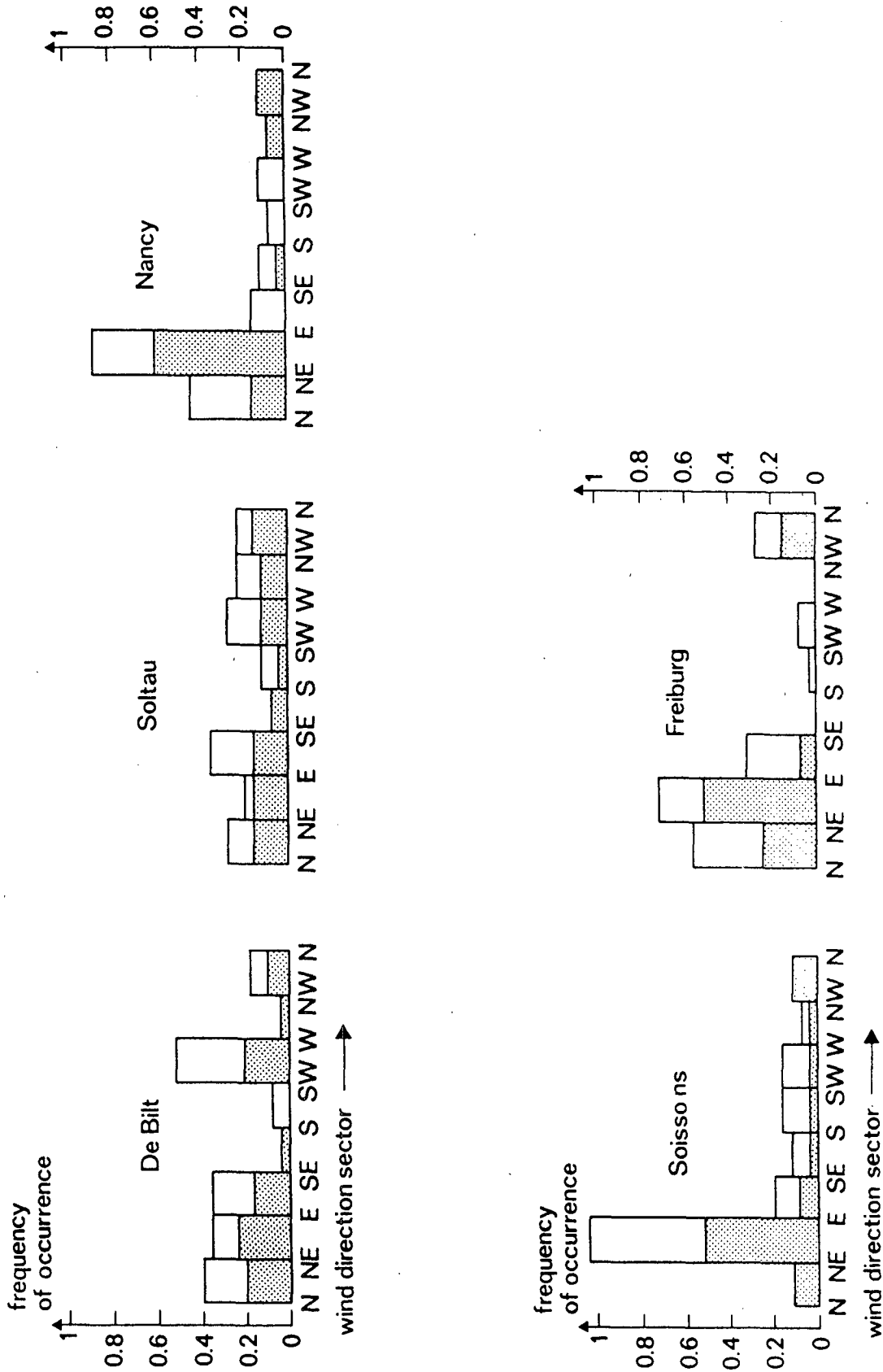


FIG. 3. Origin of surface and 850 mb trajectories. The frequency of occurrence of surface trajectories is shaded. Superimposed are the data for the 850 mb trajectories.

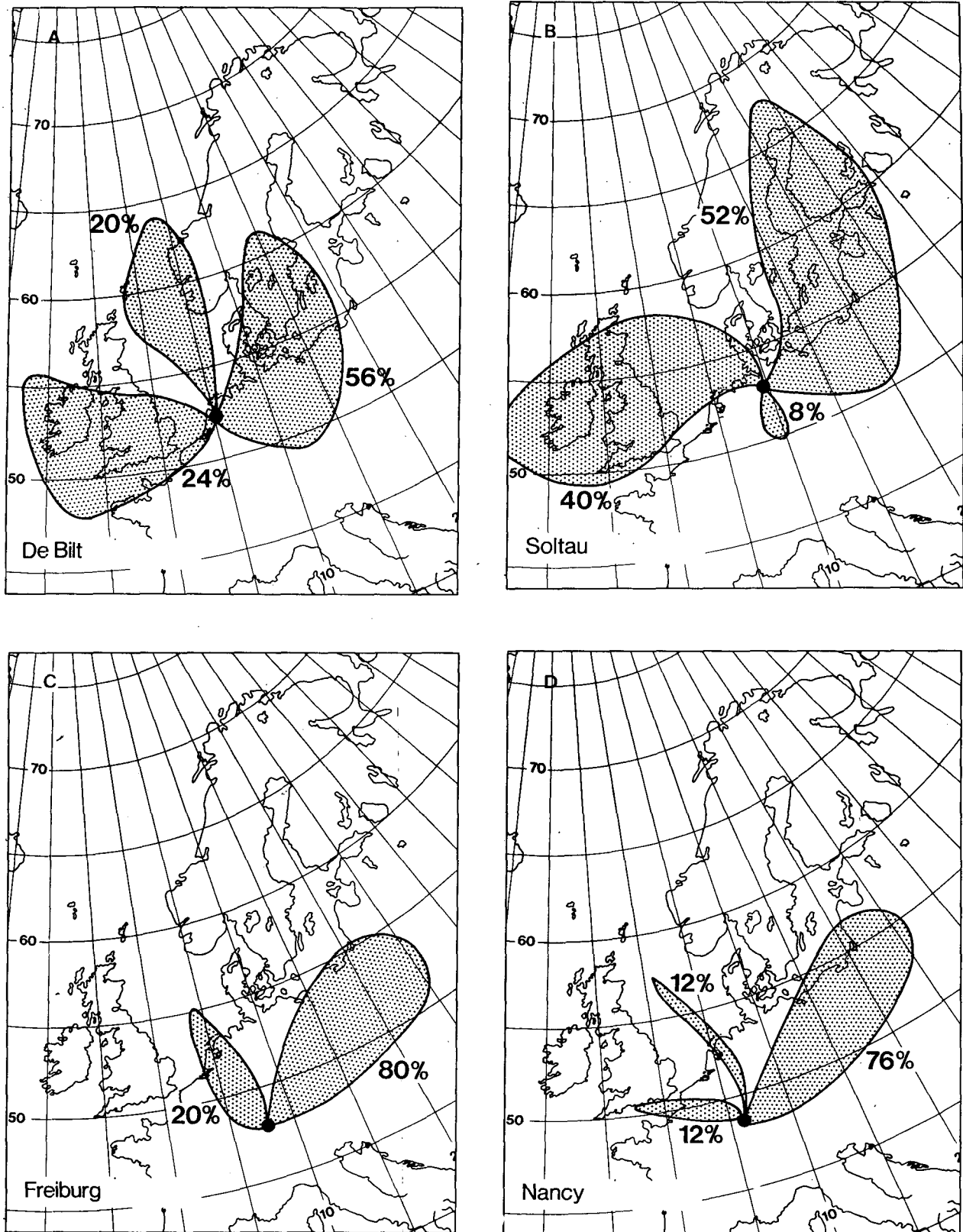


FIG. 4. Envelopes of groups of surface trajectories for (a) De Bilt, (b) Soltau, (c) Freiburg, (d) Nancy and (e) Soissons. The numbers denote the percentage of the total of (25) trajectories.

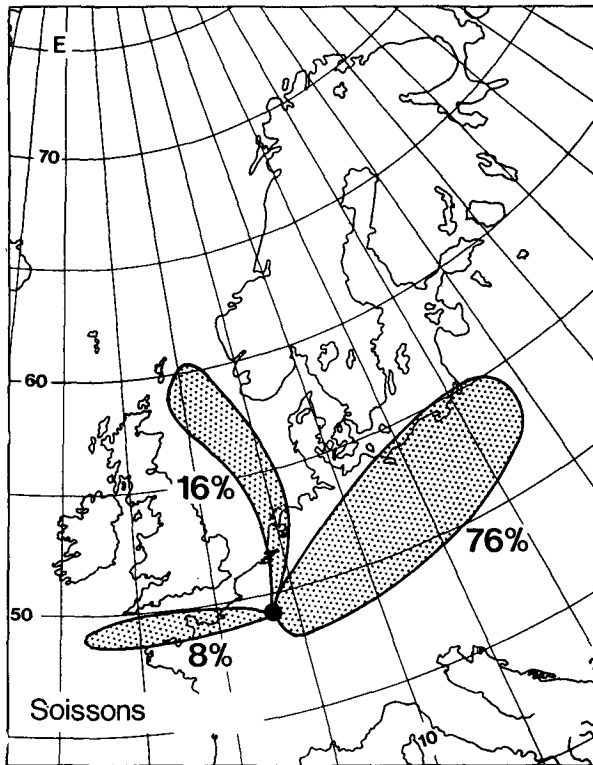


FIG. 4. (Continued)

variation for each of the trajectories was plotted. An example is shown in Fig. 5 for the trajectories leading to Freiburg. The average values were used in the photochemical model described in Part II for the trajectories over land. Because of the relatively small diurnal variation in air temperature over a water surface, the land-based mixing height values are not applicable to trajectories transversing the Baltic, the North Sea, the Bay of Biscay and the North Atlantic. A constant mixing height between 100 to 200 m over water was assumed.

From the results for the first ten episodes, and given the similarity of all selected episodes, an average mixed-layer height variation as depicted in Fig. 5 was adopted for the remaining episodes. This seems useful as a first-

TABLE 5. Classes of coherence and stagnancy for the 1000 and 850 mb trajectories ending at given locations.

Location	Coherence (C)			Stagnancy (S)		
	Good	Moderate	Poor	High	Moderate	Low
Soissons	12	5	8	6	3	16
Nancy	11	5	9	8	3	14
Freiburg	12	4	9	9	4	12
Soltau	10	8	7	4	2	19
de Bilt	10	7	8	3	5	17
All stations	9	8	8	5	7	12

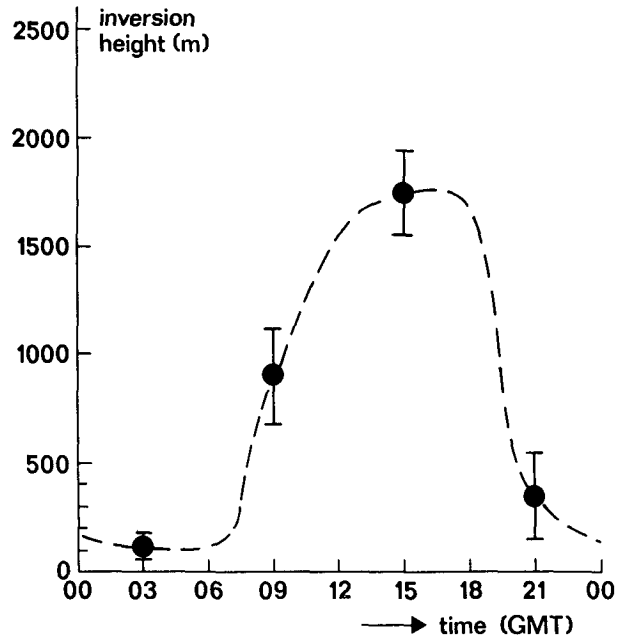


FIG. 5. The average diurnal variation of mixing height along the trajectories reaching Freiburg during episodes of warm, sunny, summer days (ten cases).

order approach for use in the Part II photochemical model.

b. Diurnal variation of temperature and humidity along surface trajectories

Similar considerations to those just described apply to the diurnal variation of temperature and humidity along the surface trajectories. Average diurnal variations of air temperature and relative humidity, determined for the first ten episodes, are shown in Figs. 6 and 7, respectively. The diurnal variation of relative humidity altered from 35% to 75% and was largely determined by the variation in temperature. The variation in water vapor content is (not surprisingly) much less than expected along the trajectory of a traveling air parcel. As noted before, for the mixed layer, the mean diurnal temperature and humidity values for the 25 episodes have been used in the Part II model calculations.

c. Clouds

The determination of trajectories for the first ten episodes from surface weather maps offered the opportunity for examining cloud observations at synoptic stations along and near the trajectories. Given the conditions for the selection of episodes, the weather was predominantly cloudless. Where clouds appeared, the overall cloudiness was mainly negligible. Most observations reported $\frac{1}{8}$ - $\frac{3}{8}$ cumulus, sometimes $\frac{7}{8}$ trans-

parent cirrus was recorded, and occasionally $\frac{5}{8}$ - $\frac{7}{8}$ thin altocumulus.

With regard to the model in Part II, photochemical processes are unlikely to be influenced by $\frac{0}{8}$ - $\frac{2}{8}$ cloudiness (>93% sunshine) and only slightly for cases when insolation is reduced by 25%–30%. In the selected cases, the weather was on one or two occasions cloudy ($\frac{3}{8}$ - $\frac{7}{8}$) or overcast ($\frac{8}{8}$) on the last day of the 72-h trajectory.

5. O₃ concentrations observed during episodes

Useful O₃ observations were available from Cabauw, close to de Bilt, in the Netherlands. Measurements of O₃ concentration are summarized in Table 6. Generally, the values were recorded for 2–3 hours around 1600 UTC. Sometimes, however, they were recorded between 1600 and 1900 UTC, or from 1400 to 1700 UTC. Measurements from the Cabauw tower (25 km SW of de Bilt in a rural area), were made at three heights, 3 m, 100 m and 200 m. Data listed are for episodes 1, 7–9 and 11–25. No measurements were available for the other episodes.

The relationship between the height at which the mean afternoon ozone peak was recorded, the geographical sector from which the surface and 850 mb trajectories originate, the stagnant character of the weather condition and the air mass properties (i.e., its continental or maritime character) are examined.

Often ozone concentrations are biased by local road traffic and industrial sources, and it may be more appropriate to consider ozone concentrations at the higher elevations as more representative of conditions associated with the path of the air parcel. The afternoon

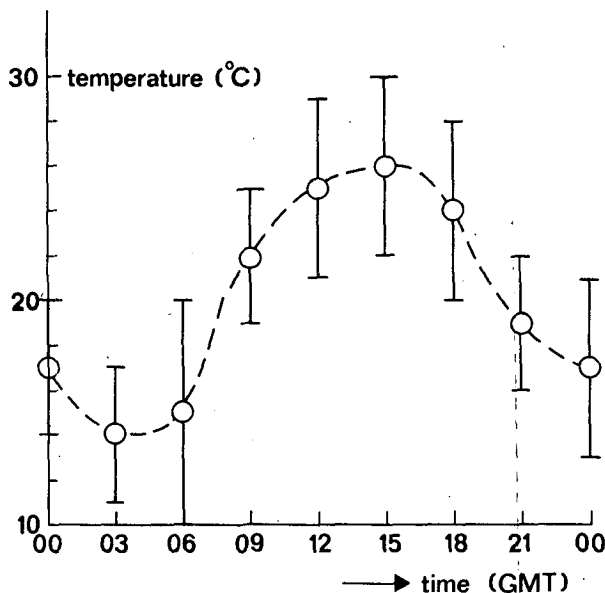


FIG. 6. The average diurnal variation of air temperature along trajectories reaching Nancy, during episodes of warm sunny summer days (ten cases).

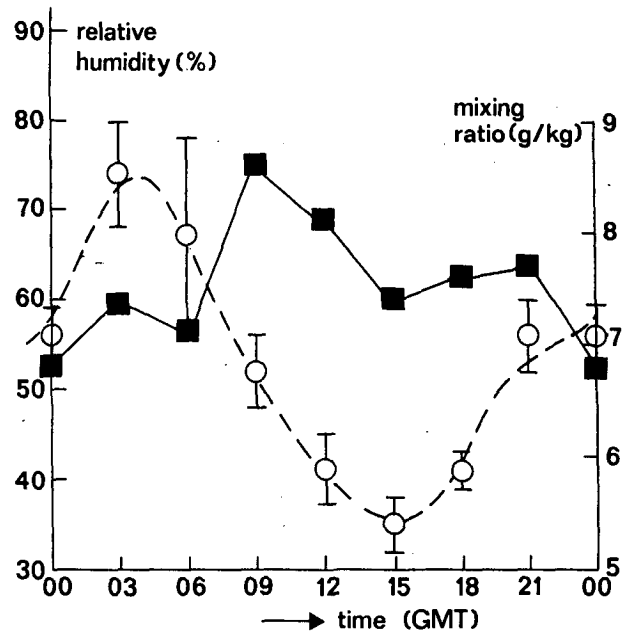


FIG. 7. The average diurnal variation of relative humidity (○) and mixing ratio (■), along trajectories reaching Nancy during episodes of warm sunny summer days (ten cases).

data when the boundary layer is well mixed, shown in Table 6, indicate, however, that the 3 m observations correlate well (correlation coefficient = 0.79) with those at 200 m. In only nine cases is the difference in concentration larger than $35 \mu\text{g m}^{-3}$, which, given the accuracy of measurement, would be considered as significantly different. The 200 m ozone concentrations have been categorized into four ranges, as shown in Table 7. The lowest range reflects the natural background concentration normally associated with relatively clean, rural areas. Additional photochemical activity increases the ozone concentration to the higher values.

The following inferences are drawn from Table 7:

- The lowest concentrations ($<80 \mu\text{g m}^{-3}$)¹ correspond to a nonstagnant weather condition with advection from the west sector.
- The highest concentrations ($>160 \mu\text{g m}^{-3}$), which are the majority, are mainly associated with continental advectons which have easterly or southerly components.
- The moderate and predominantly stagnant weather conditions were all associated with high ozone concentrations, ($>160 \mu\text{g m}^{-3}$). However, seven (i.e., 50% of the cases) nonstagnant weather conditions also gave rise to high O₃ concentrations. Thus, a stagnant weather situation is not a necessary condition for high O₃ concentrations.

¹ For comparison purposes, a conversion of $2 \mu\text{g m}^{-3} = 1 \text{ ppb}$ for ozone concentrations may be used.

TABLE 6. Observed afternoon maximum ozone concentrations ($\mu\text{g m}^{-3}$) at three heights during episodes at Cabauw (The Netherlands).

Episode	Date	3 m	100 m	200 m	Episode	Date	3 m	100 m	200 m
1	6 May 1976	190	232	—	17	10 July 1982	105	105	105
	7 May 1976	172	203	—		11 July 1982	185	175	170
	8 May 1976	255	253	—		12 July 1982	195	180	170
	9 May 1976	190	220	—		13 July 1982	200	185	170
7	29 May 1978	97	60	85	18	9 Sept. 1982	—	90	85
	30 May 1978	135	90	120		10 Sept. 1982	120	165	155
	31 May 1978	156	100	140		11 Sept. 1982	90	120	115
	1 June 1978	225	140	185		12 Sept. 1982	80	160	210
8	27 July 1978	140	90	115	19	14 Sept. 1982	—	140	—
	28 July 1978	205	135	190		15 Sept. 1982	—	260	—
	29 July 1978	245	145	210		16 Sept. 1982	—	155	—
	30 July 1978	240	155	220		17 Sept. 1982	230	235	215
9	19 Aug. 1978	95	165	60	20	17 June 1983	100	90	100
	20 Aug. 1978	120	200	75		18 June 1983	120	105	230
	21 Aug. 1978	75	140	60		19 June 1983	110	95	105
	22 Aug. 1978	75	135	55		20 June 1983	155	135	145
11	11 May 1980	145	150	130	21	9 July 1983	165	170	175
	12 May 1980	155	155	140		10 July 1983	180	180	180
	13 May 1980	145	145	130		11 July 1983	200	200	195
	14 May 1980	140	140	125		12 July 1983	155	155	160
12	22 July 1980	135	150	150	22	13 July 1983	110	110	120
	23 July 1980	135	145	150		14 July 1983	130	130	130
	24 July 1980	120	140	145		15 July 1983	210	210	215
	25 July 1980	165	180	180		16 July 1983	220	220	205
13	12 Aug. 1981	100	105	120	23	16 Aug. 1983	110	110	110
	13 Aug. 1981	130	135	160		17 Aug. 1983	20	40	50
	14 Aug. 1981	270	265	320		18 Aug. 1983	105	105	105
	15 Aug. 1981	215	315	250		19 Aug. 1983	200	215	210
14	3 Sept. 1981	165	95	105	24	24 Aug. 1983	130	135	135
	4 Sept. 1981	105	105	120		25 Aug. 1983	150	165	165
	5 Sept. 1981	125	120	140		26 Aug. 1983	100	100	100
	6 Sept. 1981	195	185	220		27 Aug. 1983	70	70	70
15	31 May 1982	210	205	185	25	28 Aug. 1983	90	75	75
	1 June 1982	290	285	260		29 Aug. 1983	85	90	90
	2 June 1982	205	200	180		30 Aug. 1983	150	150	145
	3 June 1982	250	230	215		31 Aug. 1983	195	205	190
16	7 June 1982	185	190	180					
	8 June 1982	160	160	145					
	9 June 1982	120	120	105					
	10 June 1982	160	150	135					

• The two lower ranges of values ($<160 \mu\text{g m}^{-3}$) were all associated with nonstagnant weather conditions.

• The percentages of maritime and continental trajectories associated with the four categories of ozone levels are

Trajectory	Ozone class ($\mu\text{g m}^{-3}$)			
	<80	80–159	160–200	>200
Percent maritime advection	100%	33%	40%	33%
Percent continental advection	0%	67%	60%	67%

It seems reasonable to conclude that air of continental origin is more likely to be associated with a high ozone level than maritime air.

6. Conclusions

• During spells of dry, warm and sunny weather, conducive to photochemical activity, large quasi-stationary anticyclonic systems were situated over West or Central Europe and Scandinavia. The presence of anticyclonic circulations in the investigated period was more frequent than usual.

• 72-h back-trajectories for the two more northern European receptor locations chosen are more or less evenly distributed over all wind directions and tend to pass over less densely populated, rural, or maritime areas.

• The trajectories for Freiburg originate predominantly from NE directions, then pass over populated and industrialized areas and are generally more stagnant than those examined for other locations.

TABLE 7. Values of 200 m ozone concentrations and the associated episodes. For each episode, the sector in which the surface and 850 mb trajectories originate, the stagnancy and the maritime or continental character of the advected air are given.

O ₃ Conc. ($\mu\text{g m}^{-3}$)	Episode No.	Level (mb)		Stagnancy	Air mass
		1000	850		
<80	9	WSW	WSW	—	m
	24	NNW	NNW	—	m
80–159	11	NNE	NNE	—	c
	16	NNW	NNW	—	c
	20	NNW	NNE	—	m
160–200	7	ENE	ESE	—	c
	12	ESE	WSW	—	m
	17	NNE	ENE	—	c
	21	NNW	ESE	mod	m
	25	ENE	ENE	+	c
>200	1	ENE	ENE	—	c
	18	ESE	ESE	mod	c
	13	WSW	WSW	—	m
	14	ENE	ESE	mod	c
	15	ESE	ESE	—	c
	18	WSW	WSW	—	m
	19	WSW	SSW	mod	c
	22	WNW	WSW	mod	m
	23	ESE	WSW	+	c

- The determination of air mass trajectories only has physical significance when trajectories determined at the 850 mb altitude, coincide reasonably well with surface trajectories. In roughly one-third of the cases examined, the coherence of trajectories was so low that the association with air pollution source areas is uncertain.

- The diurnal variation of temperature, humidity and mixed-layer height during the first ten episodes was pronounced. The daily maximum temperature varied between 17°C and 33°C with an average value of 26°C, whilst the minimum temperature had a range from 8°C to 21°C with an average value of 14°C. The average daily maximum mixed layer height was 1700 m. The nocturnal inversion height was about 100 m. It is expected that these conditions were also representative of the remaining 15 episodes.

- For most of the episodes examined, cloud cover was negligible, though during the night and the early morning, fog or fog patches were frequently observed.

- A preliminary analysis of recorded ozone data in the Netherlands (Cabauw) during the 25 episodes examined, suggests a relationship between locally measured peak ozone values and the origin of the air mass. The higher ozone values are related to trajectories of continental origin and to weather situations of a stagnant character.

- For the majority of the episode days examined, ozone concentrations (Cabauw) were well above the natural background level of 40–80 $\mu\text{g m}^{-3}$.

Acknowledgments. Ozone data were made available by the Institute for Public Health and Environmental

Hygiene (RIVM) and by the Institute for Applied Research (TNO). The study was sponsored by Shell Internationale Petroleum Maatschappij B.V.

REFERENCES

- Becker, H. K., U. Schurath, H. W. Georgii and M. Deimel, 1979: Untersuchungen über die Ausbildung von Oxidanten als Folge der Luftverunreinigung in der BDR. *Umweltbundesmat.*
- Cox, R. A., A. E. J. Eggleton, R. G. Derwent, J. G. Lovelock and O. H. Pack, 1976: Long-range transport of photochemical ozone in northwestern Europe. *Nature*, **225**, 118–121.
- Derwent, R. G., and O. Hov, 1982: The potential for secondary pollutant formation in the atmospheric boundary layer in a high-pressure situation over England. *Atmos. Environ.*, **16**, 655–665.
- Eliassen, A., and J. Saltbones, 19xx: Modelling of long-range transport of sulphur over Europe: A two-year model run and some model experiments. *Atmos. Environ.*, **17**, 1457–1473.
- , O. Hov, I. S. A. Isaksen, J. Saltbones and F. Stordal, 1982: A Lagrangian long-range transport model with atmospheric boundary layer chemistry. *J. Appl. Meteor.*, **21**, 1645–1661.
- Guicherit, R., and H. van Dop, 1977: Photochemical production of ozone in Western Europe (1971–1975) and its relation to meteorology. *Atmos. Environ.*, **11**, 145–155.
- , Ed., 1978: Photochemical smog formation in the Netherlands. TNO, P.O. Box 214, 2600 AE Delft, The Netherlands.
- Hess, P., and H. Brezowski, 1969: Katalog der Groswetterlagen Europa's. *Berichte des Deutschen Wetterdienstes*. Nr. 113. Frankfurter Strasse 135 6050 Offenbach a.M., Federal Republic of Germany.
- Holzworth, G. C., 1967: Mixing depths, wind speed and air pollution potential for selected location in the USA. *J. Appl. Meteor.*, **6**, 1039–10xx.
- Hov, O., A. Eliassen, J. Saltbones, I. S. A. Isaksen and F. Stordal, 1983: Regional model for oxidants: The Norwegian Lagrangian long range transport model with atmospheric boundary-layer chemistry. *Procs. of the EPA-OECD International Conference on Long Range Transport Models of Petrochemical Oxidants and their Precursors*. EPA Report No. 600/9-84-006, Triangle Park, NC, 94–152.
- Johnson, A. H., and T. J. Siccamo, 1983: Acid deposition and forest decline. *Environ. Sci. Technol.*, **17**, 294.
- Miller, P. R., and J. R. McBride, 1975: Effects of air pollutants on forests. (c.f., responses of plants to air pollution. Mudd, J. B., Kozkonski, T. T., Eds.) Academic Press, 196–296.
- Pack, D. H., G. J. Ferber, J. L. Huffter, K. Tekgadas, J. K. Angell, W. H. Hoecker and L. Machta, 1978: Meteorology of long-range transport. *Atmos. Environ.*, **12**, 425–444.
- Reiff, J., D. Blaauboer, H. A. R. de Bruin, A. P. van Ulden and G. Cats, 1984: An air mass transformation model for short-range weather forecasting. *Mon. Wea. Rev.*, **112**, 393–412.
- Rodhe, H., P. Crutzen and A. Vanderpol, 1982: Formation of sulfuric and nitric acid in the atmosphere during long-range transport. *Tellus*, **33**, 132–141.
- Rottenheim, J. W., K. A. Brice and K. G. Anlauf, 1984: Discussions of a Lagrangian trajectory model describing long-range transport of oxides of nitrogen, the incorporation of PAN in the chemical mechanism, and supporting measurements of PAN and nitrate species at rural sites in Ontario. *Canada. Atmos. Environ.*, **18**, 2609–2619.
- Schjoldager, J., H. Dovland, P. Greunfelt and J. Saltbones, 1981: Photochemical oxidants in northwestern Europe 1976–1979; a pilot study. NILU-rapp. nr. 19/81, 24–31. [Nilu, P.O. Box 130 2001 Lillestrom, Norway.]
- Selby, K., 1987: A modeling study of atmospheric transport and photochemistry in the mixed layer during anticyclonic episodes in Europe. Part II: Calculations of photo-oxidant levels along air trajectories. *J. Climate Appl. Meteor.*, **26**, 1317–1338.
- Smith, W. H., 1981: Air pollution and forests. Springer Verlag.
- Ulrich, B., R. Mayer and T. K. Khanna, 1980: Chemical changes due to acid precipitation in a loss-derived soil in Central Europe. *Soil Sci.*, **130**, 193.